Ain Shams Engineering Journal (2016) xxx, xxx–xxx

Ain Shams University

Ain Shams Engineering Journal

www.elsevier.com/locate/asej
www.sciencedirect.com

Entropy generation analysis for viscoelastic MHD flow over a stretching sheet embedded in a porous medium

S. Baag [a,*], S.R. Mishra [b], G.C. Dash [b], M.R. Acharya [a]

[a] Department of Physics, College of Basic Science and Humanities, O.U.A.T, Bhubaneswar 751003, Odisha, India
[b] Department of Mathematics, I.T.E.R, Siksha 'O' Anusandhan University, Khandagiri, Bhubaneswar 751030, Odisha, India

Received 30 July 2015; revised 16 September 2015; accepted 25 October 2015

KEYWORDS

Entropy;
MHD;
Viscoelastic liquid;
Darcy dissipation;
Stretching surface;
Kummer's function

Abstract In this paper it is intended to analyse entropy generation by applying second law of thermodynamics to magnetohydrodynamic flow, heat and mass transfer of an electrically conducting viscoelastic liquid (Walters B') past on a stretching surface, taking into account the effects of Joule dissipation, viscous dissipation and Darcy dissipation, and internal heat generation. The boundary layer equations are solved analytically by using Kummer's function. The entropy generation has been computed considering Darcy dissipation besides viscous and Joule dissipation. Results for some special cases of the present analysis are in good agreement with the existing literature. Increase in viscoelastic and magnetic parameter reduces the velocity. Increase in elastic parameter causes a greater retardation in the velocity. Presence of porous matrix enhances temperature whereas increase in Prandtl number decreases the temperature. One striking result of the present study is that Darcy dissipation favours higher level entropy generation in all the cases except the flow of liquid with low thermal diffusivity assuming the process to be irreversible.

1. Introduction

The fluid flow over a stretching sheet is important in many practical applications such as extrusion of plastic sheets, paper production, glass blowing, metal spinning, polymers in metal spring processes, the continuous casting of metals, drawing plastic films and spinning of fibres, all involve some aspects of flow over a stretching sheet or cylindrical fibre (Paullet and Weidman [1]). The quality of the final product depends on the rate of heat transfer at the stretching surface.

Literature survey indicates that interest in the flows over a stretched surface has grown during the past decades. The problem of stretching surface with constant surface temperature was analysed by Crane [2]. Later, the stretching sheet flow has been studied by several researchers for the sole effects of rotation, velocity and thermal slip conditions, heat and mass

* Corresponding author. Mobile: +91 9040258068.
E-mail addresses: sbaag22@gmail.com (S. Baag), satyaranjan_mshr@yahoo.co.in (S.R. Mishra).
Peer review under responsibility of Ain Shams University.

ELSEVIER Production and hosting by Elsevier

http://dx.doi.org/10.1016/j.asej.2015.10.017

Nomenclature

A	constant	B	constant
B_0	uniform magnetic field strength	B_r	Brinkman number
C_p	specific heat of the solid	D	molecular diffusivity
D_a	Darcy number	d	characteristic length
f	dimensionless function	H_a	Hartmann number
K'	permeability of the medium	K_P	porosity parameter
K	thermal conductivity of the fluid	M	Kummer's function
Mn	magnetic parameter	P_r	Prandtl number
Q	heat source/sink parameter	q_r	radiative heat flux
q_w	wall heat flux	R_e	elastic parameter
R	radiation parameter	S_c	Schmidt number
T	non-dimensional temperature	t'	time
t	non-dimensional time	T_∞	temperature far from sheet
T'	temperature of the field	T_w	wall temperature
ρ	density of the fluid	υ	kinematic coefficient of viscosity
k_1	absorption coefficient	σ^*	Stefan–Boltzmann constant
σ	electrical conductivity	τ_w	wall shear stress
k_0	dimensionless elastic parameter	m_w	rate of mass flux
q	heat generation coefficient	r	plate temperature parameter
s	plate concentration parameter		

transfer, chemical reaction, MHD, suction/injection, different non-Newtonian fluids or possible combinations of these effects ([3–8]).

Chamkha [9] studied the MHD flow of uniformly stretched vertical permeable surface in the presence of heat generation/absorption and a chemical reaction. Ishak et al. [10] investigated theoretically the unsteady mixed convection boundary-layer flow and heat transfer due to a stretching vertical surface in a quiescent viscous and incompressible fluid. Sammer [11] investigated the heat and mass transfer over an accelerating surface with heat source in the presence of magnetic field. Wang [12] studied the stagnation flow towards a shrinking sheet. Akbar et al. [13] investigated the dual solutions in MHD stagnation-point flow of a Prandtl fluid impinging on a shrinking sheet. Akbar et al. [14] have also studied MHD stagnation point flow of Carreau fluid towards a permeable shrinking sheet. Partial slip effect on non-aligned stagnation point nanofluid over a stretching convective surface has been investigated by Nadeem et al. [15].

Naseem and Khan [16] investigated boundary-layer flow past a stretching plate with suction, heat and mass transfer and with variable conductivity. Cortell [17] also reported the flow and heat transfer of a fluid through porous medium over a stretching surface with internal heat generation. Combined effects of magnetic field and partial slip on obliquely striking rheological fluid over a stretching surface have been investigated by Nadeem et al. [18]. Akbar et al. [19] have studied the numerical analysis of magnetic field effects on Eyring–Powell fluid flow towards a stretching sheet. Free convective heat and mass transfer for MHD fluid flow over a permeable vertical stretching sheet in the presence of the radiation and buoyancy effects has been investigated by Rashidi et al. [20,21].

The main concern in the present study is to account for the entropy generation/minimization on the heat transfer process. One of the most important characteristics of the medium in thermodynamics is the entropy. In an adiabatic process, the entropy either increases or remains unchanged (second law of thermodynamics). Entropy generation is closely associated with the thermodynamic irreversibility. Irreversibility analysis in a couple stress film flow along an inclined heated plate with adiabatic free surface has been studied by Adesanya and Makinde [22]. Recently, inherent irreversibility in Sakiadis flow of nanofluids has been investigated by Makinde et al. [23]. Mahamud and Fraser [24–26] applied the second law of thermodynamics to convective heat transfer in non-Newtonian fluid flow through a channel. Akbar [27] has studied entropy generation analysis for a CNT Suspension Nanofluid in Plumb Ducts with Peristalsis. He has also investigated Peristaltic flow with thermal conductivity of H_2O + Cu nanofluid and entropy generation [28]. Entropy generation and energy conversion rate for the peristaltic flow in a tube with magnetic field has also been investigated by Akbar [29]. Makinde [30] has investigated entropy analysis for MHD boundary layer flow and heat transfer over a flat plate with a convective surface boundary condition. Entropy analysis for an unsteady MHD flow past a stretching permeable surface in nano-fluid has been studied by Abolbashari et al. [31]. Chemical reaction effect on MHD free convective surface over a moving vertical plane through porous medium has been studied by Tripathy et al. [32].

Moreover, Aiboud et al. [33] studied the second law analysis of laminar fluid flow in a heated channel with hydromagnetic and viscous dissipation effect. They made an entropy analysis for viscoelastic MHD flow over a stretching surface [34].

The growing need for chemical reaction and hydrometallurgical industries requires the study of heat and mass transfer with chemical reaction. There are many transport processes that are governed by the combined action of buoyancy forces

due to both thermal and mass diffusion in the presence of chemical reaction effect. These processes are observed in the nuclear reactor safety and combustion systems, solar collectors, as well as metallurgical and chemical engineering.

All the studies referred above do not include the effect of mass diffusion in the presence of diffusing species though it is a common phenomenon, and occur simultaneously with heat transfer. Further, the novelty of the present study is to account for the effect of Joulian dissipation in addition to viscous dissipation on the entropy generation. Another important aspect of the present study is the flow of viscoelastic fluid on a stretching surface embedded in a uniformly porous saturated medium. We have applied Darcy's linear model to account for the permeability of the porous medium. One more significance of the present study is the entropy generation analysis which is one of the most important characteristics of the medium depending upon the quantities of heat added. We have considered here additional heat due to (i) magnetic field (Joulian dissipation) and (ii) porous medium (Darcy dissipation). Thus, the present study brings to its fold many previous studies as particular cases. In particular, the case of Aiboud and Saouli [34] has been discussed by ignoring the effects of (i) Joule's dissipation parameter and (ii) permeability parameter. Therefore, the generalization aims at developing a mathematical model to account for (i) the loss of energy while dealing with MHD flows, (ii) the resistance offered by the porous matrix embedding the stretching surface, and (iii) the effect of diffusing species.

The method of solution of the coupled nonlinear equation is quite interesting. The solution is based upon a choice of a function satisfying the boundary conditions but is valid to a class of viscoelastic fluid for which elastic parameter $R_c \neq 1$. Upon introducing the stream function the order of the equation is increased from third to fourth order. The solution can be obtained by applying Von Mises transformation Anes [35] which reduces the order to third order i.e. the order of the original governing equation. However, we have solved governing equations analytically by using hypergeometric function (Kummer's function).

2. Formulation of the problem

A steady laminar, incompressible electrically conducting, viscoelastic fluid flow caused by a stretching surface embedded in a porous medium in the presence of a uniform transverse magnetic field in cartesian coordinate (x, y) where x-axis is taken in the direction of main flow along the plate and y-axis is normal to the plate, is considered (see Fig. 1).

The boundary-layer equations for a steady two-dimensional Darcian flow of viscoelastic liquid of Walters B' model with short relaxation time following Schlichting [36] are given by

$$\frac{\partial u}{\partial x}+\frac{\partial v}{\partial y}=0, \tag{1}$$

$$u\frac{\partial u}{\partial x}+v\frac{\partial u}{\partial y}=\upsilon\frac{\partial^2 u}{\partial y^2}-\frac{\sigma B_0^2 u}{\rho}-\frac{\upsilon}{K_P'}u-\frac{k_0}{\rho}\left(\frac{\partial}{\partial x}\left(u\frac{\partial^2 u}{\partial y^2}\right)+\frac{\partial^3 u}{\partial y^3}-\frac{\partial u}{\partial y}\frac{\partial^2 u}{\partial x\partial y}\right), \tag{2}$$

$$\rho C_p\left(u\frac{\partial T}{\partial x}+v\frac{\partial T}{\partial y}\right)=K\frac{\partial^2 T}{\partial y^2}+q(T-T_\infty), \tag{3}$$

$$u\frac{\partial C}{\partial x}+v\frac{\partial C}{\partial y}=D\frac{\partial^2 C}{\partial y^2}, \tag{4}$$

The boundary conditions are

$$\left.\begin{array}{ll} u=u_p=\lambda x,\ v=0,\ T=T_p(x)=A\left(\frac{x}{l}\right)^r+T_\infty, & \\ C=C_p(x)=B\left(\frac{x}{l}\right)^s+C_\infty, & \text{at } y=0,\\ u=0,\ \frac{\partial u}{\partial y}=0,\ T\to T_\infty,\ C\to C_\infty, & \text{as } y\to\infty. \end{array}\right\} \tag{5}$$

3. Solution of the flow field

Eq. (1) is satisfied if we choose a dimensionless stream function

$$u=\frac{\partial\psi}{\partial y},\quad v=-\frac{\partial\psi}{\partial x}. \tag{6}$$

Introducing the similarity transformations

$$\eta=y\sqrt{\frac{\lambda}{\upsilon}},\ \psi(x,y)=x\sqrt{\upsilon\lambda}f(\eta), \tag{7}$$

and substituting in (2), we get

$$f'''+ff''-f'^2-R_c\{2f'f'''-f''^2-ff^{iv}\}-\left(Mn+\frac{1}{K_P}\right)f'=0, \tag{8}$$

where f is the dimensionless stream function and η is the similarity variable, $R_c=k_0\lambda/\mu$, the viscoelastic parameter, $Mn=\sigma B_0^2/\rho\lambda$, the magnetic parameter and $K_p=K_p^*/\rho\lambda$, the permeability parameter.

The corresponding boundary conditions are as follows:

$$f(0)=0,\ f'(0)=1,\ f'(\infty)=0,\ f''(\infty)=0. \tag{9}$$

Following Rajgopal [37], the solution of (8) with boundary conditions (9) can be written as

$$f(\eta)=\frac{1-e^{-\alpha\eta}}{\alpha},\ \alpha>0 \tag{10}$$

where $\alpha=\sqrt{\frac{1+Mn+1/K_p}{1-R_c}}$; $R_c\neq 1$ and $R_c<1$ provided

(i) $R_c\neq 1$

(ii) $R_c<1$

Violation of condition (i) leads to non-existence of $f(\eta)$ which restricts our discussion to the choice of viscoelastic liquid for which $k_0\lambda\neq\mu$ i.e. the dynamic viscosity must not be equal to the product of elasticity and stretching rate. The violation of condition (ii) is restricted by the choice of fluid model i.e. Walters B' which is valid for slightly elastic liquid.

The local skin friction coefficient or the frictional drag coefficient is given by

$$C_f=\frac{\tau_w}{\mu\lambda x\sqrt{\frac{\lambda}{\upsilon}}}=\alpha$$

where τ_w is the wall shearing stress on the sheet.

4. Heat transfer analysis

Introducing non-dimensional quantities $\theta(\eta)=\frac{T-T_\infty}{T_p-T_\infty}$, $P_r=\mu C_p/K$, $\beta=\frac{qv}{\rho C_p}$ and using (7), Eq. (3) becomes

$$\theta'' + P_r f\theta' + P_r(\beta - rf')\theta = 0, \tag{11}$$

with the boundary conditions

$$\theta(0) = 1,\ \theta(\infty) = 0. \tag{12}$$

Introducing the variable $\xi = \frac{P_r e^{-\alpha\eta}}{\alpha^2}$ Eq. (11) is transformed to

$$\xi\frac{d^2\theta}{d\xi^2} + \left(1 - \frac{P_r}{\alpha^2} + \xi\right)\frac{d\theta}{d\xi} - \left(r - \frac{\beta}{\alpha^2}\right)\theta = 0, \tag{13}$$

with the boundary conditions

$$\theta(\xi = \frac{P_r}{\alpha^2}) = 1,\ \theta(\xi = 0) = 0. \tag{14}$$

Using confluent hypergeometric function we get,

$$\theta(\xi) = \left(\frac{\alpha^2\xi}{P_r}\right)^{a+b}\frac{M(a+b-r, 1+2b, -\xi)}{M(a+b-2, 1+2b, -P_r/\alpha^2)}, \tag{15}$$

where $a = P_r/2\alpha^2$, $b = \sqrt{(P_r)^2 - 4\alpha^2\beta}/2\alpha^2$ and $M(\alpha_1, \alpha_2; x)$ denotes the Kummer's function

$$M(\alpha_1, \alpha_2; x) = \sum_{n=0}^{\infty}\frac{(\alpha_1)_n}{(\alpha_2)_n}\frac{x^n}{n!},\ \alpha_2 \neq 0, -1, -2\ldots \tag{16}$$

where $(\alpha)_n$ denotes the Pochhammer symbol defined in terms of the gamma function.

The temperature profile in terms of η is obtained as

$$\theta(\eta) = e^{-\alpha(a+b)\eta}\frac{M\left(a+b-2, 1+2b, \frac{-P_r}{\alpha^2}e^{-\alpha\eta}\right)}{M\left(a+b-2, 1+2b, \frac{-P_r}{\alpha^2}\right)}. \tag{17}$$

The wall temperature gradient or the local Nusselt number is given by

$$-\theta'(0) = \alpha(a+b) - \frac{P_r}{\alpha}\frac{M\left(a+b-1, 2b+2, \frac{-P_r}{\alpha^2}\right)}{M\left(a+b-2, 1+2b, \frac{-P_r}{\alpha^2}\right)}.$$

5. Mass transfer analysis

Introducing the similarity variable $\varphi(\eta) = \frac{C-C_\infty}{C_p-C_\infty}$, and using (6), in Eq. (4) we get,

$$\varphi'' + S_c f\varphi' - S_c f'\varphi = 0, \tag{18}$$

with the boundary conditions

$$\begin{aligned} &\varphi' = -1 \quad \text{at} \quad \eta = 0,\\ &\varphi \to 0 \quad \text{at} \quad \eta \to \infty. \end{aligned} \tag{19}$$

Again introducing a new variable $\zeta = -\frac{S_c}{\alpha^2}e^{-\alpha\eta}$, Eq. (18) becomes

$$\zeta\frac{d^2\varphi}{d^2\zeta} + \left[\left(1 - \frac{S_c}{\alpha^2}\left(\alpha^2 - M^2 - \frac{1}{K_p}\right)\right) - \zeta\right]\frac{d\varphi}{d\zeta} + s\varphi = 0, \tag{20}$$

The corresponding boundary conditions are

$$\varphi(\zeta = 0) = 0,\ \varphi'\left(\zeta = -\frac{S_c}{\alpha^2}\right) = -\frac{\alpha}{S_c}. \tag{21}$$

The exact solution of Eq. (20) subject to the boundary condition (21) is given by

$$\varphi(\eta) = \frac{e^{-\alpha\eta}{}_1F_1(\gamma-2; 1+\gamma; -\frac{S_c e^{-\alpha\eta}}{\alpha^2})}{\alpha\gamma_1F_1(\gamma-2; 1+\gamma; -\frac{S_c}{\alpha^2}) - \frac{S_c}{\alpha}\frac{\gamma-2}{(1+\gamma)}{}_1F_1\left(\gamma-1; 2+\gamma; -\frac{S_c}{\alpha^2}\right)}, \tag{22}$$

$$\gamma = \frac{S_c}{\alpha^2}\left(\alpha^2 - M - \frac{1}{K_p}\right).$$

The wall concentration gradient or the local Sherwood number is given by

$$-\varphi'(0) = \frac{\alpha_1F_1\left(\gamma-2; 1+\gamma; -\frac{S_c}{\alpha^2}\right) + \frac{S_c}{\alpha}{}_1F_1\left(\gamma-1; \gamma+2; -\frac{S_c}{\alpha^2}\right)}{\alpha\gamma_1F_1\left(\gamma-2; 1+\gamma; -\frac{S_c}{\alpha^2}\right) - \frac{S_c}{\alpha}\frac{\gamma-2}{(1+\gamma)}{}_1F_1\left(\gamma-1; 2+\gamma; -\frac{S_c}{\alpha^2}\right)}.$$

6. Entropy generation analysis

The local volumetric rate of entropy generation in the presence of magnetic field is given by

$$\begin{aligned} E_G = {} & \frac{k}{T_\infty^2}\left(\left(\frac{\partial T}{\partial x}\right)^2 + \left(\frac{\partial T}{\partial y}\right)^2\right) + \frac{D}{C_\infty}\left(\left(\frac{\partial C}{\partial x}\right)^2 + \left(\frac{\partial C}{\partial y}\right)^2\right)\\ & + \frac{D}{T_\infty}\left(\frac{\partial T}{\partial x}\frac{\partial C}{\partial x} + \frac{\partial T}{\partial y}\frac{\partial C}{\partial y}\right) + \frac{\mu}{T_\infty}\left(\frac{\partial u}{\partial y}\right)^2 + \frac{\sigma B_0^2}{T_\infty}u^2\\ & + \frac{\mu}{T_\infty K_p'}u^2 \end{aligned} \tag{23}$$

The contribution of all the parameters to the entropy generation is shown in Eq. (23). The first term on the right hand side of Eq. (23) is the entropy generation due to the heat transfer across a finite temperature difference, the second term is the local entropy due to viscous dissipation, the third term is due to the Lorentz force, and the final term is the local entropy generation due to porous matrix. The entropy generation number is

$$N_s = \frac{E_G}{E_{G0}}, \tag{24}$$

where E_{G0} is the characteristic entropy generation rate. i.e. N_s is defined as dividing the local volumetric entropy generation rate E_G to a characteristic entropy generation rate E_{G0}. From the given boundary condition the characteristic entropy generation rate is

$$E_{G0} = \frac{k(\Delta T)^2}{d^2T_\infty^2}. \tag{25}$$

Using Eqs. (7), (17) and (23), the entropy generation number is given by

$$\begin{aligned} N_s = {} & \frac{r^2}{X^2}\theta^2(\eta) + \mathrm{Re}_d\theta'^2(\eta) + \mathrm{Re}_d\frac{B_r}{\Omega}f'^{\prime 2}(\eta) + \frac{B_r(H_a^2 + 1/D_a)}{\Omega}f'^2\\ & + \frac{s^2}{X^2}\lambda_1\phi^2(\eta) + \mathrm{Re}_d\lambda_2\phi'^2(\eta)\\ & + \lambda_3\left(\frac{rs}{X^2}\theta(\eta)\phi(\eta) + \mathrm{Re}_d\theta'(\eta)\phi'(\eta)\right), \end{aligned} \tag{26}$$

where Re_d and B_r are the Reynolds number and the Brinkman number respectively. Ω and H_a are respectively the dimensionless temperature and Hartman number. These are defined as

$$\mathrm{Re}_d = \frac{u_d d}{\nu},\ B_r = \frac{\mu u_p^2}{k\Delta T},\ \Omega = \frac{\Delta T}{T_\infty},\ H_a = B_0 d\sqrt{\frac{\sigma}{\mu}},\ \frac{1}{D_a} = \frac{d^2}{K_p^*},$$
$$X = \frac{x}{d},\ \lambda_1 = \frac{DT_\infty}{kC_\infty}\left(\frac{\Delta C}{\Delta T}\right)^2,\ \lambda_2 = \frac{DT_\infty^2}{kC_\infty}\left(\frac{\Delta C}{\Delta T}\right)^2,$$
$$\lambda_3 = \frac{DT_\infty}{k}\left(\frac{\Delta C}{\Delta T}\right).$$

7. Results and discussion

The following discussion centres round to bring out the effect of controlling parameters on volumetric rate of entropy generation besides citing the result of the previous author [34] as a particular case. The striking feature of the velocity profiles, for both longitudinal and transverse components is of two layer character.

Figs. 2 and 3 show the longitudinal velocity profiles for viscous ($R_c = 0$) and viscoelastic ($R_c \neq 0$) liquid in the presence of porous medium ($K_p = 0.5$) and in the absence ($K_p = 100$), ([34]).

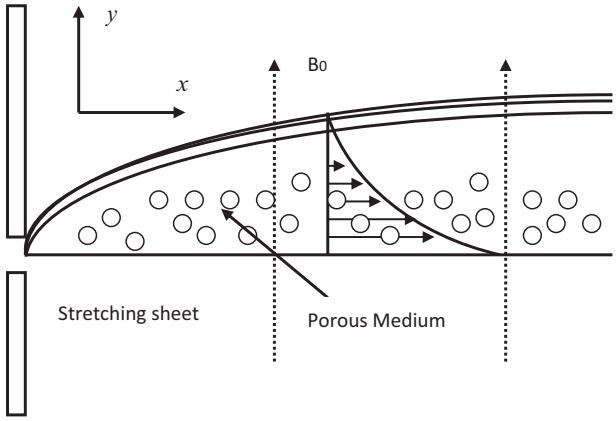

Figure 1 Flow geometry.

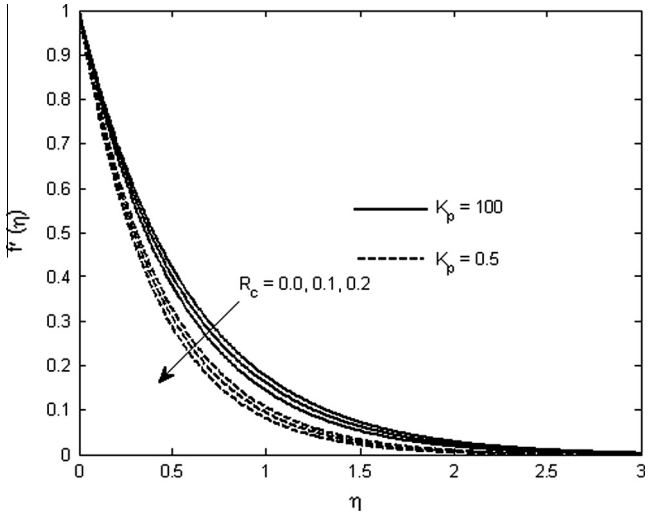

Figure 2 Effect of R_c and K_p on longitudinal velocity for $Mn = 2$.

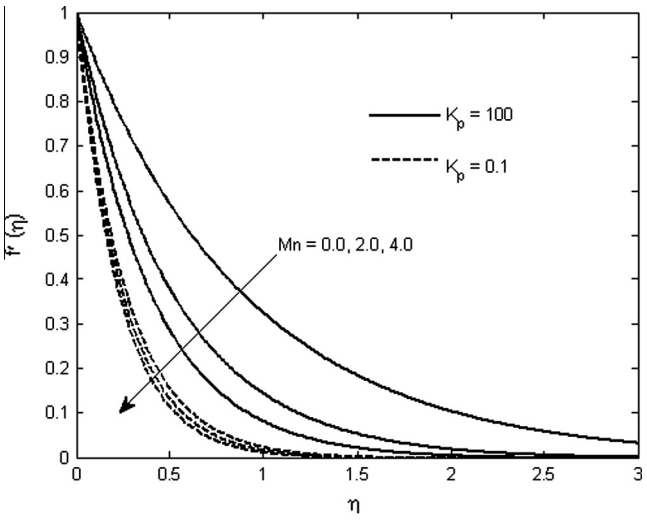

Figure 3 Effect of Mn and K_p on transverse velocity for $R_c = 0.2$.

It is to note that increase in viscoelastic and magnetic parameter reduces the velocity uniformly. This observation agrees well with [34] and it is also remarked that the presence of porous matrix reduces the velocity further. The increase in Mn imposes greater Lorentz force, a resistive force of electromagnetic origin, causes a reduction in the velocity. Moreover, in case of elastic liquid we cannot neglect strain; however, small it may be, besides strain rate for viscous liquid, as it is responsible for the recovery to the original state and for the reverse flow that follows the removal of stress. Hence, in viscoelastic liquid there is a degree of recovery from the strain when the stress is removed. The increase in elastic parameter leads to greater degree of recovery which causes a greater retardation in the velocity [34]. Moreover, two-layer character is being exhibited by the velocity profiles due to magnetic field, permeability and elastic parameters.

Figs. 4 and 5 show the retardation of transverse velocity due to increase in the magnetic parameter and elastic

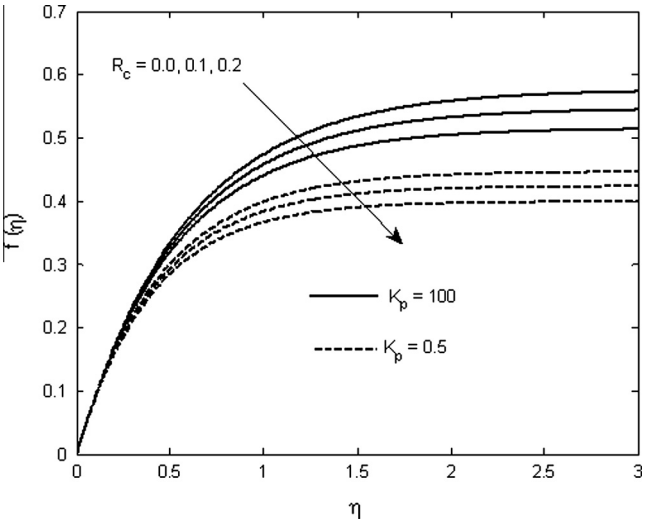

Figure 4 Effect of R_c and K_p on transverse velocity for $Mn = 2$.

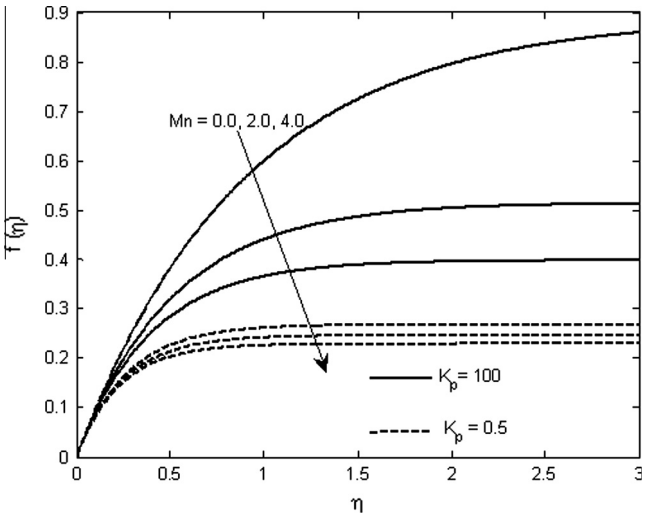

Figure 5 Effect of Mn and K_p on longitudinal velocity for $R_c = 0.2$.

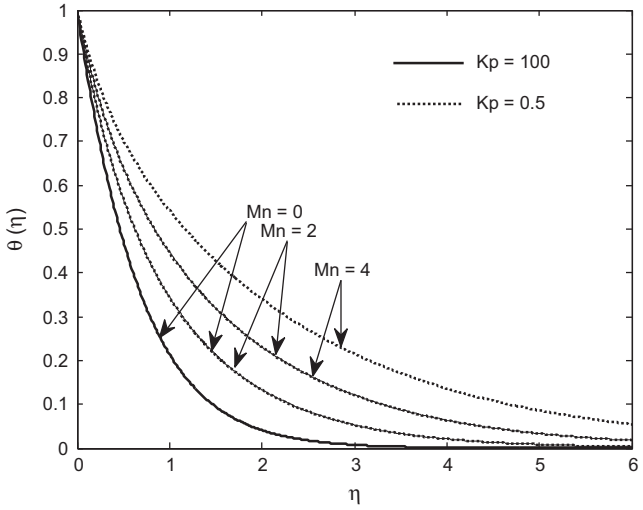

Figure 7 Effect of Mn and K_p on temperature profile for $P_r = 2, R_c = 0.2, \beta = 0.1, r = 1$.

parameter and it is further reduced by the presence of porous medium. It is remarked that the effect of all the parameters on both the components remains the same. On careful observation it is further revealed that in the presence of porous material, the compression of profiles is well marked in both the cases but it is significant in the presence of magnetic field.

From Figs. 6–8 it is observed that presence of porous matrix enhances the temperature at all points which contribute to spreading of thermal boundary-layer to a larger domain whereas, increase in Prandtl number decreases the temperature. The Prandtl number is a relative measure of the mechanism of heat conduction and viscous stresses. For gases P_r is of the order of unity which implies that heat conduction and viscosity of the gas enjoy same priority. In the present case we have considered the value of $P_r > 1$ i.e. for liquid. From the profiles it is clear that temperature decreases with an increase in P_r implies flow of liquids with low thermal diffusivity and high viscous stresses which causes a fall of temperature

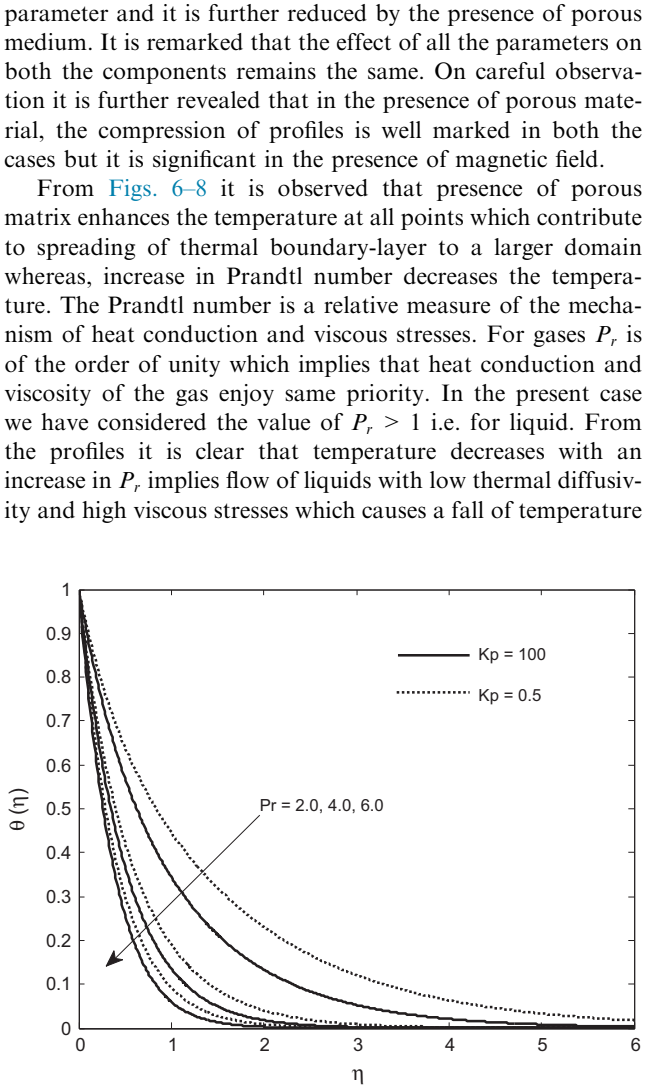

Figure 8 Effect of R_c and K_p on temperature profile for $P_r = 2, Mn = 2, \beta = 0.1, r = 1$.

Figure 6 Effect of P_r and K_p on temperature Profile for $Mn = 2, R_c = 0.2, \beta = 0.1, r = 1$.

in the thermal boundary-layer, generates thinner boundary-layer. It is further to note that magnetic parameter and elastic parameter accelerate the temperature at all points. This seems quite justified because of the resistive force due to interaction of magnetic field and release of strain energy for the recovery and reverse flow on removal of stress, causing retardation in the velocity which has been discussed in Figs. 2 and 3. Hence, both the resistive forces cause a retardation of velocity thereby enhancing the temperature at all points. The same observation made by Chen [38] is "Viscoelasticity will produce a rise in the temperature profiles for Walters' liquid B' " and the rise of temperature with Mn is also indicated. This is also in good agreement with [34].

Figs. 9 and 10 show the effects of heat source/sink parameter. It is seen that temperature increases with the increase in source strength and the reverse effect is observed with an increase in r the power index characterizing the temperature

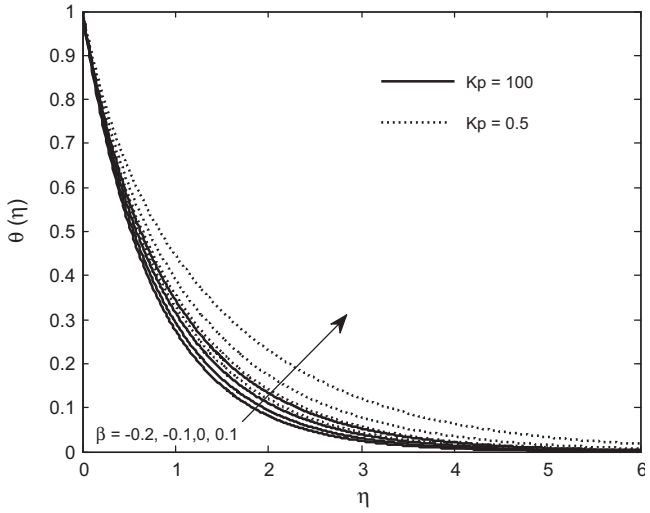

Figure 9 Effect of β (source/sink) on temperature profile for $P_r = 2, Mn = 2, R_c = 0.2, r = 1$.

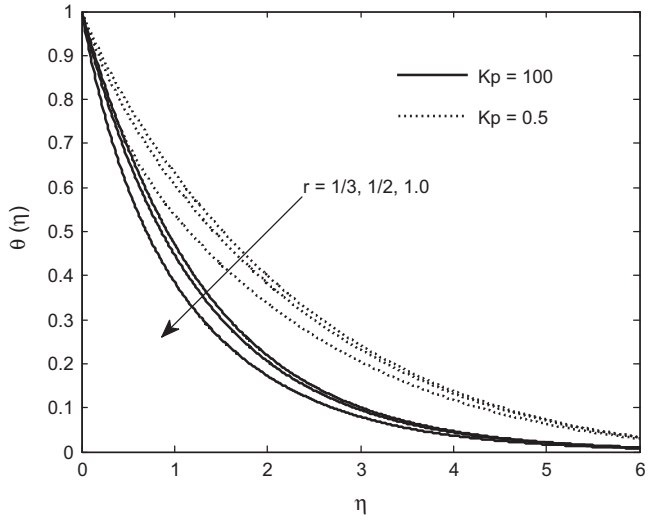

Figure 10 Effect of r on temperature profile for $P_r = 2, Mn = 2, \beta = 0.2, R_c = 0.2$.

variation. This is in good agreement with [34]. It is further noticed that sink decreases the temperature and presence of porous medium ($K_p = 0.5$) increases the temperature in the presence of source/sink.

Fig. 11 depicts the concentration distribution for various values of parameters. From curves I and II it is seen that heavier species decreases the concentration without magnetic field and porous medium. Curves I and III show that magnetic parameter increases the concentration distribution significantly at all points. Curves III and IV show that the presence of porous medium increases the concentration level at all points also. Curves (IV, VIII) and (III, VII) claim that for higher index, s, the concentration decreases irrespective of presence or absence of porous medium. The same observation was made earlier in respect of temperature also.

Thus, it is concluded that heavier species and higher power index of plate concentration distribution cause a fall

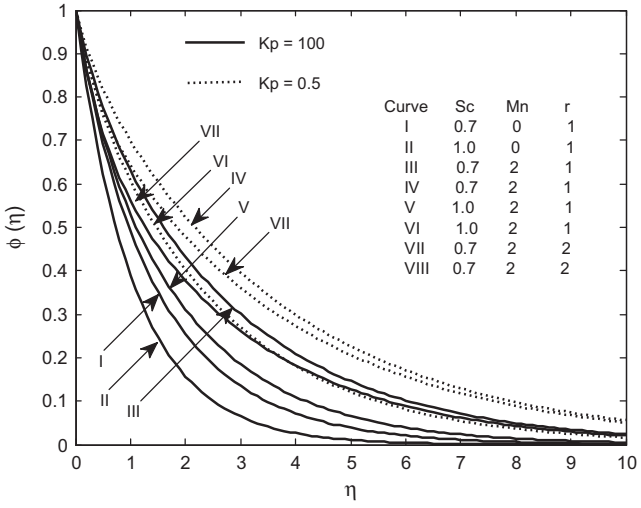

Figure 11 Effect of S_c, Mn, K_p and r on concentration profiles.

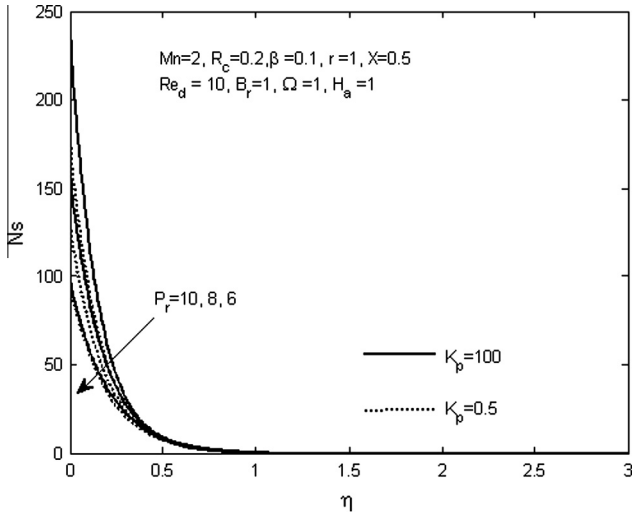

Figure 12 Effect of P_r and K_p on the entropy generation number for $s = \lambda_1 = \lambda_2 = \lambda_3 = 0$.

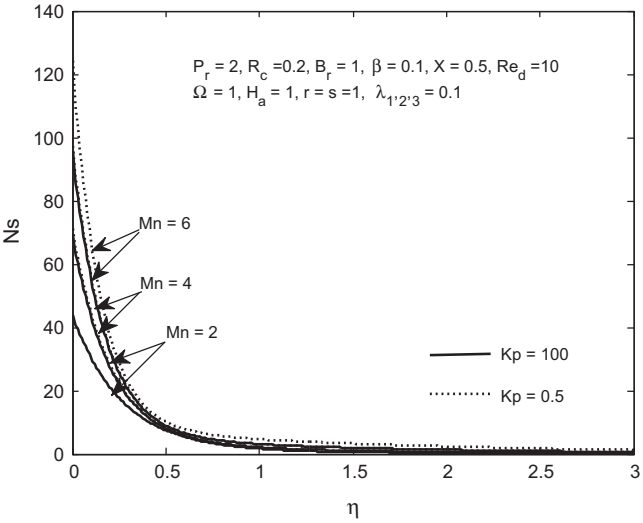

Figure 13 Effect of Mn and K_p on the entropy generation number.

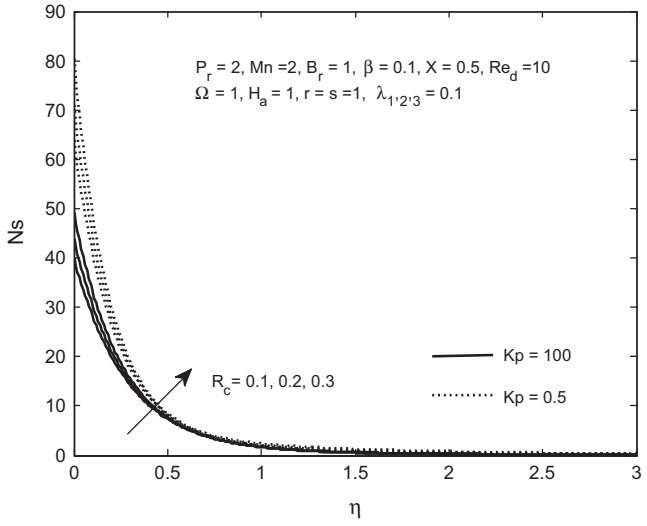

Figure 14 Effect of R_c and K_p on the entropy generation number.

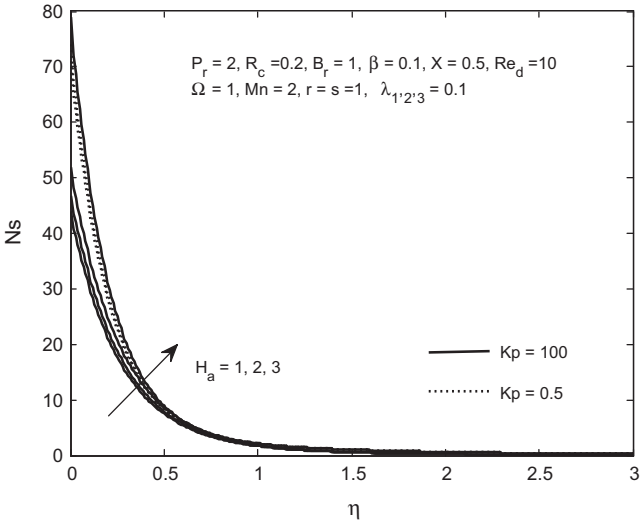

Figure 16 Effect of H_a and K_p on the entropy generation number.

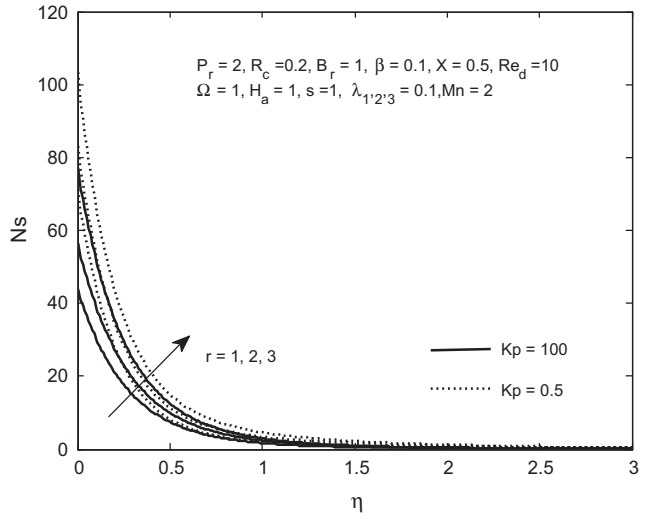

Figure 15 Effect of r and K_p on the entropy generation number.

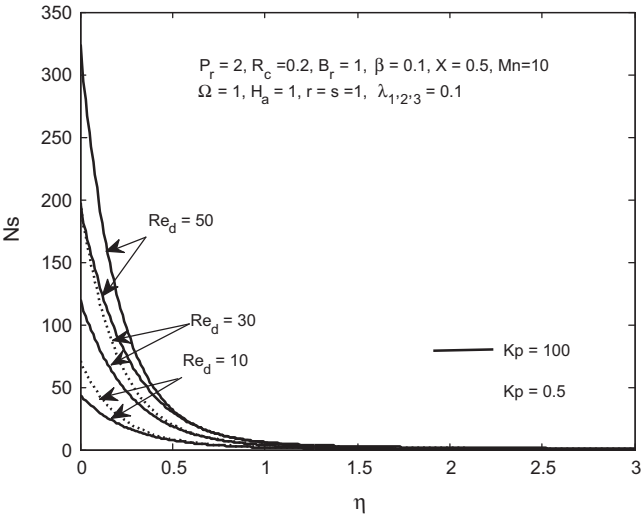

Figure 17 Effect of Re_d and K_p on the entropy generation number.

in concentration whereas, under the influence of Lorentz force and permeability of the medium the concentration level increases. The rise in concentration level may be attributed to the resistance offered by Lorentz force and presence of porous medium creating an impasse to the flow.

Now, one of the most important characteristics of the medium i.e. volumetric entropy generation in the presence of magnetic field and porous medium is to be discussed. While discussing the effect of entropy generation following Woods [39] we have disregarded the contribution due to heat at constant pressure since the present discussion is confined to incompressible liquid only. Besides the contribution of viscous dissipation and Joulian dissipation considered by [34] we have considered the Darcy dissipation term. Figs. 12–14 show the effects of P_r, Mn and R_c on the entropy generation. The higher Prandtl number fluid and magnetic parameter generate higher entropy and the presence of Darcy dissipation reduces it. This shows that presence of porous medium acts adversely for higher Prandtl fluid flow in generating higher entropy.

The role of elastic parameter is interesting. It exhibits two layer characters with higher entropy generation in the presence of porous medium and the role of elastic parameter is same as that of Prandtl number and magnetic parameter.

Figs. 15–17 exhibit the effects of plate temperature parameter r, the Hartmann number H_a and Reynolds number Re_d. On careful observation it is revealed that:

(i) The roles of r and H_a are same as Mn only with lower start-up at the plate.
(ii) The role of Reynolds number is also to generate the higher entropy with one distinction contributing substantially in comparison with other parameters.

Table 1 Values of skin friction coefficient ($f''(0)$), Nusselt number ($-\theta'(0)$) and Sherwood number ($-\phi'(0)$) for $r = s = 1$.

Mn	R_c	P_r	β	S_c	K_p	$f''(0)$	$-\theta'(0)$	$-\phi'(0)$
1	0.1	0.7	0.1	0.7	100	−1.49443	−0.134778	0.045939
2	0.1	0.7	0.1	0.7	100	−1.82878	−0.131969	0.02873
2	0.2	0.7	0.1	0.7	100	−1.93972	−0.129429	0.024877
2	0.2	7	0.1	0.7	100	−1.93972	1.00566	0.024877
2	0.2	0.7	0.2	0.7	100	−1.93972	−0.134037	0.024877
2	0.2	0.7	0.1	0.22	100	−1.93972	−0.129429	0.002993
2	0.2	0.7	0.1	0.7	0.5	−2.5	−0.113953	0.012976
2	0.2	7	0.1	0.7	0.5	−2.5	0.72805	0.012976

To sum up, inclusion of Darcy dissipation in the process of entropy generation in the present study favours higher entropy level in all the curves baring liquid with higher Prandtl number (liquid with low thermal diffusivity). Another striking feature is that the entropy generation is positive in all the cases assuring the process is irreversible. The process is irreversible in case of viscous liquid (Pai [40]). The present study assures the irreversibility in case of viscoelastic liquid with higher level entropy generation on the bounding surface in the presence of porous medium contributing Darcy dissipation.

Finally, typical variables, the local skin friction coefficient in terms of $f''(0)$, local Nusselt number i.e. wall temperature gradient $-\theta'(0)$ and local Sherwood number i.e. the wall concentration gradient $-\phi'(0)$ for various parameters are shown in Table 1. An increase in Mn and R_c decreases the skin friction as well as Sherwood number whereas P_r is to increase the Nusselt number in the absence of porous matrix. Further, in the presence of porous matrix increase in P_r decreases the Nusselt number.

Rate of mass transfer at the surface is measured evaluating $-\phi'(0)$. The species considered are hydrogen ($S_c = 0.22$) and water vapour ($S_c = 0.7$) in air medium for both destructive and constructive reaction rates. Following facts are evident from the tabulated values (Table 1). Heavier species in both the presence/absence of porous matrix increases the rate of mass transfer.

8. Conclusion

The reduction of velocity due to viscoelasticity of the liquid in the presence of magnetic field is favoured in the presence of porous medium resulting in a thinner boundary-layer, whereas opposite effect is observed in case of thermal and concentration boundary-layers. Heavier species and higher concentration index contribute to thinner boundary-layer. The present study assures the irreversibility in case of viscoelastic liquid with higher entropy generation. Also heavier species is favourable to increase the concentration gradient.

References

[1] Paullet J, Weidman. Analysis of stagnation point flow forward a stretching sheet. Int J Non-linear Mech 2008;42:1048–91.
[2] Crane LJ. Flow past a stretching plane. Jape Math Phys (ZAMP) 1970;21:645–7.
[3] Ishak A, Nazar R, Pop I. Heat transfer over a stretching surface with variable heat flux in micropolar fluids. Phys Lett A 2008;372:559–61.
[4] Ishak A, Nazar R, Arifin NM, Pop I. Mixed convection of the stagnation point flow towards a stretching vertical permeable sheet. Malaysian J Math Sci 2007;2:217–26.
[5] Ishak A, Nazar R, Pop I. Mixed convection boundary layers in the stagnation point flow towards a stretching vertical permeable sheet. Mechanica 2006;41:509–18.
[6] Yao S, Fang T, Zhong Y. Heat transfer of a generalized stretching/shrinking wall problem with convection boundary conditions. Commun Nonlinear Sci Numer Simul 2011;16:752–60.
[7] Quasim M, Hayat T, Obaidat S. Radiation effect on the mixed convection flow of a viscoelastic fluid along an inclined stretching sheet. Z Naturforsch 2012;67:195–202.
[8] Hayat T, Quasim M, Mesloub S. MHD flow and heat transfer over a stretching sheet with Newtonian heating with slip condition. Int J Numer Methods Fluid 2011;66:963–75.
[9] Chamkha AJ. MHD flow of a uniformly stretched permeable surface in the presence of heat generation/absorption and a chemical reaction. Int Comn Heat Mass Transfer 2003;30:413–22.
[10] Ishak A, Nazar R, Pop I. Unsteady mixed convection boundary layer flow due to a stretching vertical surface. Arabian J Soc Eng 2006;31:165–82.
[11] Sammer AA. Heat and mass transfer over an accelerating surface with heat source in presence of magnetic field. IJTAM 2009;4:281–93.
[12] Wang CY. Stagnation flow towards a shrinking sheet. Int J Nonlinear Mech 2008;43:377–82.
[13] Akbar NS, Khan ZH, Haq RU, Nadeem S. Dual solutions in MHD stagnation-point flow of Prandtl fluid impinging on shrinking sheet. Appl Math Mech 2014;35(7):813–20.
[14] Akbar NS, Nadeem S, Haq Rizwan Ul, Ye Shiwei. MHD stagnation point flow of Carreau fluid toward a permeable shrinking sheet: dual solutions. Ain Shams Eng J 2014;5:1233–9.
[15] Nadeem S, Rashidi MM, Akbar NS. Partial slip effect on non-aligned stagnation point nanofluid over a stretching convective surface. Chin Phys B 2015;24(1):014702.
[16] Naseem A, Khan N. Boundary layer flow past a stretching plate with suction and heat transfer with variable conductivity. Int J Eng Mater Sci 2000;7:51–3.
[17] Cortell R. Flow and heat transfer of a fluid through a porous medium over a stretching surface with internal heat generation/absorption and suction/blowing. Fluid Dyn Res 2005;37:231–45.
[18] Nadeem S, Rashid MM, Akbar NS. Combined effects of magnetic field and partial slip on obliquely striking rheological fluid over a stretching surface. J Magn Magn Mater 2015;378:457–62.
[19] Akbar NS, Ebaid A, Khan ZH. Numerical analysis of magnetic field effects on Eyring–Powell fluid flow towards a stretching sheet. J Magn Magn Mater 2015;382:355–8.
[20] Rashidi MM, Rostami B, Navid F, Abbasbandy S. Free convective heat and mass transfer for MHD fluid flow over a permeable vertical stretching sheet in the presence of the radiation and buoyancy effects. Ain Shams Eng J 2014;5(3):901–12.
[21] Rashidi MM, Vishnu Ganesh N, Abdul Hakeem AK, Ganga B. Buoyancy effect on MHD flow of nanofluid over a stretching

Please cite this article in press as: Baag S et al., Entropy generation analysis for viscoelastic MHD flow over a stretching sheet embedded in a porous medium, Ain Shams Eng J (2016), http://dx.doi.org/10.1016/j.asej.2015.10.017

sheet in the presence of thermal radiation. J Mol Liq 2014;198:234–8.
[22] Adesanya SO, Makinde OD. Irreversibility analysis in a couple stress film flow along an inclined heated plate with adiabatic free surface. Physica A 2015;432:222–9.
[23] Makinde OD, Khan WA, Aziz A. On inherent irreversibility in Sakiadis flow of nanofluids. Int J Exergy 2013;13(2):159–74.
[24] Mahmud S, Fraser RA. The second law analysis in fundamental convective heat transfer problems. Int J Therm Sci 2003;42:177–86.
[25] Mahmud S, Fraser RA. Thermodynamic analysis of flow and heat transfer inside channel with two parallel plates. Energy 2002;2:140–6.
[26] Mahmud S, Fraser RA. Inherent irreversibility of channel and pipe flows for non-Newtonian fluids. Int Comm Heat Mass Transfer 2002;29:577–87.
[27] Akbar NS. Entropy generation analysis for a CNT suspension nanofluid in plumb ducts with peristalsis. Entropy 2015;17 (3):1411–24.
[28] Akbar NS, Raza M, Ellahi R. Peristaltic flow with thermal conductivity of H_2O + Cu nanofluid and entropy generation. Result Phys 2015;5:115–24.
[29] Akbar NS. Entropy generation and energy conversion rate for the peristaltic flow in a tube with magnetic field. Energy 2015;82:23–30.
[30] Makinde OD. Entropy analysis for MHD boundary layer flow and heat transfer over a flat plate with a convective surface boundary condition. Int J Exergy 2012;10(2):142–54.
[31] Abolbashari MH, Freidoonimehr N, Nazari F, Rashidi MM. Entropy analysis for an unsteady MHD flow past a stretching permeable surface in nano-fluid. Powder Technol 2014;267:256–67.
[32] Tripathy RS, Dash GC, Mishra SR, Baag S. Chemical reaction effect on MHD free convective surface over a moving vertical plane through porous medium. Alexandria Eng J 2015; 54:673–9.
[33] Aiboud S, Saouli S, Settou N, Meza N. Second law analysis of laminar fluid flow in a heated channel with hydromagnetic and viscous dissipation effects. Appl Energy 2007;84:279–89.
[34] Aiboud S, Saouli S. Entropy analysis for viscoelastic magnetohydrodynamic flow over a stretching surface. Int J Non-Linear Mech 2010;45:482–9.
[35] William F. Anes, numerical methods for partial differential equations. New York, San Francisco: Academic Press; 1977.
[36] Schlichting H, Boundary layer theory, 6th ed., New York: Mc Graw Hill. p. 118 and 411.
[37] Rajgopal KR. On the boundary conditions for fluids of differential type. In: Sequeira A, editor. Navier–Stokes equation and related non linear problems. New York: Plenum Press; 1995. p. 273–8.
[38] Chen Chien-Hsin. On the analytic solution of MHD flow and heat transfer for two types of viscoelastic fluid over a stretching sheet with energy dissipation, internal heat source and thermal radiation. Int J Heat Mass Transfer 2010;53:4264–73.
[39] Woods LC. Thermodynamics of fluid systems. Oxford: Oxford University Press; 1975.
[40] Shih-I Pai. Viscous flow theory I – laminar flow. Princeton, New Jersey: D. Van Nostrnd Company, INC; 1956.

S.R. Mishra, Assistant Professor, Department of Mathematics, Institute of Technical Education and Research, Siksha 'O' Anusandhan University, Khandagiri, Bhubaneswar-751030, Orissa, India.

S. Baag, Assistant Professor, Department of Physics, OUAT, Bhubaneswar, India.

G.C. Dash, Professor, Department of Mathematics, Institute of Technical Education and Research, Siksha 'O' Anusandhan University, Khandagiri, Bhubaneswar-751030, Orissa, India.

Dr. M.R. Acharya, Associate Professor, Department of Physics, College of Basic Sciences and Humanities, OUAT, Bhubaneswar, Odisha, India.